HYDRATION OF NONCHARGED LIPID BILAYER MEMBRANES

Theory and Experiments with Phosphatidylethanolamines

GREGOR CEVC AND DEREK MARSH
Max-Planck-Institut für biophysikalische Chemie, Abteilung Spektroskopie, D-3400 Göttingen, Federal Republic of Germany; and Institute of Biophysics Medical Faculty and Institute Josef Stefan, University of Ljubljana, YU-6100 Ljubljana, Yugoslavia

ABSTRACT Calorimetric measurements have been made on the thermodynamics of the chain-melting phase transition of saturated diacylphosphatidylethanolamines, with chains containing 12–20 carbons, as a function of water content. The transition temperature, T_t, and the transition enthalpy, and entropy all decrease with an increase in water content; however, the effect on T_t lessens with an increase in chainlength. These results are compared with a theoretical description of lipid hydration in terms of the interlamellar water polarization (i.e., modified water structure) in the interbilayer region. The measured free energy, enthalpy and entropy of the transition and the transition temperature have an approximate hyperbolic tangent dependence on water content, $\propto \tanh (d_w/2\,\xi)$, where d_w is the interlamellar water-layer thickness and $\xi \sim 0.25$ nm is the water-order correlation length, in agreement with the theory. Auxiliary x-ray diffraction experiments yield results on the repulsive hydration forces between lipid lamellae consistent with the theory, and allow an estimate of the water orienting potential of the interface. The molecular origin of this potential is discussed in electrostatic terms, and the values of its associated molecular parameters are found to yield the right size of hydrational thermodynamic quantities. The theory thus provides an integrated, clear, and simple approach to the hydration properties of lipid membranes.

INTRODUCTION

The interaction of water molecules with the lipid polar head groups is one of the fundamental aspects of biological membrane assembly (see, e.g., reference 1). Experiments with phospholipid model membranes have shown that the degree of head group hydration affects both the membrane structure and dynamics (2). The molecular packing and chain organization (3), as well as the bilayer topography (4), and the interaction between bilayers (5–7) depend on the amount of water associated with the lipids. The chain-melting phase transition (8–12), lateral diffusion constant (13), and transformational to nonbilayer phases (11, 14) are also all dependent on water content.

Most of these previous hydration studies were performed with phosphatidylcholines only and, in addition, the physico-chemical behavior has only seldom found a quantitative theoretical description (15–18). Here we investigated the effects of head group hydration on the thermodynamics of the chain-melting phase transition of phosphatidylethanolamine bilayers and on the bilayer-bilayer interaction forces. A theory based on polarization of the water molecules by the lipid head groups is presented and is shown to be capable of explaining both the thermodynamic data and the hydration forces. This theory, which is a modification of that originally presented by Marčelja and Radić (15), provides an integrated description of water-binding hydration forces and their effects on membrane energetics.

MATERIALS AND METHODS

Lipids

1,2-dilauroyl-*sn*-glycero-3-phosphoethanolamine (DLPE), 1,2-dimyristoyl-*sn*-glycero-3-phosphoethanolamine (DMPE), 1,2-dipalmitoyl-*sn*-glycero-3-phosphoethanolamine (DPPE), 1,2-distearoyl-*sn*-glycero-3-phosphoethanolamine (DSPE), and 1,2-diarachinoyl-*sn*-glycero-3-phosphoethanolamine (DAPE) were obtained from Fluka (Buchs, Switzerland). The purity was checked, before the experiment, after calorimetry, and after completion of the x-ray diffraction measurements, by thin-layer chromatography on silicic acid plates using the solvent system $CHCl_3$/CH_3OH/NH_4OH (65:35:5 ratio) with ninhydrin and molybdate staining. The lipids were routinely dried under vacuum (<1 N · m^{-2}, >24 h) in the presence of P_2O_5. Ampoules containing the amount of lipid needed for one experiment were sealed after drying and kept at -4°C until required.

Sample Preparation

The lipid ($\sim$ 7.5 mg) from a freshly opened ampoule was placed in the sample pan and covered with a parafilm sheet of known mass. The weight of the lipid was then accurately determined. A droplet of bidistilled water exceeding somewhat the weight needed to achieve the required water/lipid ratio was introduced into the top of the pan and its evaporation rate

was monitored. The sample was sealed at the moment at which the water mass (corrected for the evaporation losses occurring during the manipulation) gave the desired water/lipid ratio, n_w. The accuracy of n_w and its reproducibility was ±0.25 H_2O/PE. An exception was the sample with $n_w < 1$, for which repeated experiments often differed from previous ones, and complex results were found.

When the calorimetry was completed, part of the lipid was used for purity control while the remainder was transferred to the x-ray specimen holder. Here the lipid was compressed between two mica plates that were sealed with a Teflon spacer. Comparison of the calorimetric and x-ray transition temperatures indicated that no substantial water loss took place during this transfer. Some samples were preheated to $T \gtrsim 100$°C for >10 min before they were used for calorimetry. Such procedures affected only the first few temperature scans.

Differential Scanning Calorimetry

Differential scanning calorimetry (DSC) experiments were performed with a DSC-2 calorimeter (Perkin-Elmer Corp., Instrument Div., Norwalk, CT). Large volume, stainless-steel pans were used with an empty reference pan, except in the case of samples with excess water for which 50 μl of bidistilled water was used as a reference. The heating (and cooling) rates were 1.25 and 2.5 K · min^{-1} with a heat flow of 0.24 mJ · s^{-1}. At least two independent experiments were made for each value of n_w, with a minimum of five cycles between (T_t–20)°C and 100–120°C for each sample. The average values of all reproducible scans were used in determining transition enthalpies, ΔH_t, and transition temperatures, T_t. Transition enthalpies were obtained by measuring the area under the excess heat vs. temperature curves by paper weighing and the corresponding molar values were calculated from the known lipid masses.

X-ray Diffraction

Measurements were made with samples previously scanned by DSC. A Guinier camera operating under reduced pressure (2.5 · 10^3 N · m^{-2}) with a bent quartz crystal monochromator (R. Huber, 8211 Rimsting, Federal Republic of Germany) was used. The monochromator was set to isolate the CuKα_1 line (λ = 0.15405 nm). The camera was modified so as to permit continuous temperature scanning (0.1 K · min^{-1}). During the experiment the temperature of the brass sample-holder block was continuously recorded (see reference 19). Single measurements at fixed temperatures were also performed, if longer exposure times were required.

THEORY

The water binding to the phospholipid polar groups is described in terms of the (orientational) polarization of the water molecules induced by the bilayer surface, as was first done by Marčelja and co-workers (16, 17, 20, 28). The polarization of the water molecules within the interlamellar space is represented by a function $P(x)$, which varies with distance from one of the two interfacial planes that are located at positions $x_i = \pm d_w/2$ for i = 1, 2, respectively. The discrete nature of the orienting field is ignored and is replaced by its effective average (volume) density, $F_p(x)$. This effective field is the sum of all short-range electrostatic, dipolar, hydrogen bonding, and other contributions from the lipid head groups (2, 31).

The change in the free energy caused by the partial orientation of the interbilayer water, $G^{hyd}(d_w)$ is described by the free-energy terms associated with the water polarization (field), its spatial variation, which accounts for the entropic part, and the coupling between the water polarization and external orienting (polarizing) field, F_p. Formally, this gives, respectively (15, 16, 18),

$$G^{hyd}(d_w) = (2\chi)^{-1} \cdot \int \{P^2(x) + \xi^2[dP(x)/dx]^2 - 2\chi F_p(x)P(x)\} \cdot dV, \quad (1)$$

where the parameter χ is a measure of the susceptibility of the interlamellar water to the orienting field and ξ is the correlation length of the water polarization. Eq. 1 contains all the free-energy terms up to the fourth order.

Profile of the Surface-induced Water Polarization

The requirement for the free energy, Eq. 1, to be minimum leads to the Euler-Lagrange differential equation that determines the profile of the surface-induced order (i.e., of the polarization) of the interlamellar water molecules

$$P(x) = \chi F_p(x) + \xi^2 d^2P(x)/dx^2. \quad (2)$$

The orienting fields of the opposing interfaces are equal in size but opposite in sign. It is assumed that the sources of these fields (the head groups) are confined to surface planes, and since in the absence of net coulombic surface charge they create merely short-range fields, we may use

$$F_p(x) = \psi_{hyd}[\delta(x + d_w/2) - \delta(x - d_w/2)], \quad (3)$$

ψ_{hyd} denotes the interfacial hydration potential of each interface. This boundary condition is physically more realistic (18) than constraining the order parameter at the surface to remain fixed, as was done originally (15).

The boundary condition for the polarization can then be found by integrating Eq. 2 throughout the volume V, which includes the boundary, and taking the limit $V \to 0$ while keeping the surface of the boundary constant. The alternative is to treat the interface as a barrier between media with correlation lengths ξ_1 and ξ_2, and then to let $\xi_1(x < -d_w/2) = \xi_1(x > d_w/2) \to 0$ and $\xi_2 \to \xi$. In both cases the result is

$$dP(x)/dx|_{x=\pm d_w/2} = -\chi\psi_{hyd}/\xi^2, \quad (4)$$

which states that the change with distance of the water polarization at the surface is proportional to the interfacial hydration potential and to the interfacial orientational susceptibility of the water molecules.

With the above boundary conditions, the solution of Eq. 2 for the interlamellar water polarization profile is given by

$$P(x) = -[(\chi\psi_{hyd}/\xi)/\cosh(d_w/2\xi)] \sinh(x/\xi). \quad (5)$$

We see that for large values of the water-layer thickness, $d_w >> \xi$, the interfacial water polarization attains a constant value, $P(\pm d_w/2) = \mp\chi\psi_{hyd}/\xi$, which is proportional to the interfacial hydration potential and orientational susceptibility. When the interfacial separation becomes small, $d_w \to 0$, the interfacial fields screen each other and $P(\pm d_w \to 0) = \mp(\chi\psi_{hyd}/\xi)\tanh(d_w/2\xi) \to 0$. Hence the expansion implicit in Eq. 1 does not lead to a divergence at $d_w \to 0$ and can be used for all values of the interfacial separation.

This is illustrated in Fig. 1, which gives the calculated polarization profiles for hydration potential ψ_{hyd} = 0.6 V and $\chi = 8.8 \cdot 10^{-12} A \cdot s \cdot (V \cdot m)^{-1}$ (the former value corresponds to phosphatidylethanolamine bilayers in the fluid state as discussed later), and various values of the water-layer thickness. As d_w decreases so does the maximum value of the interfacial polarization, although the values of the polarization closer to the midplane (x = 0) of the water layer are higher at the closer separations.

Molecular Origin of Lipid Hydration

Detailed knowledge of the sources of the orienting field, F_p, and hence of the lipid hydration could be obtained by investigating exact interaction potentials of lipid layers with their surrounding waters. Such calculations are at present possible only with severe simplifications. We, therefore, present a very approximate picture of the (noncharged) lipid head group hydration at the molecular level based on simple electrostatic consider-

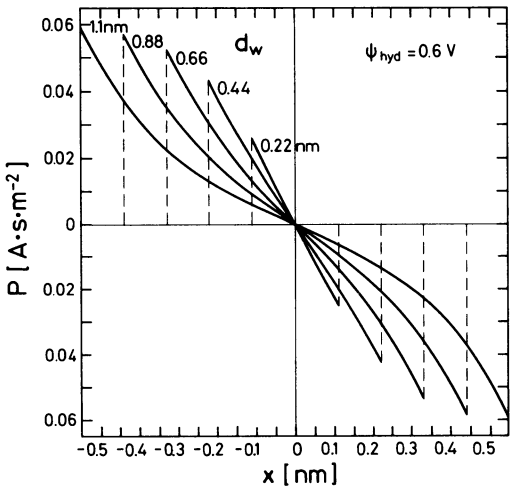

FIGURE 1 Profile of the water orientational polarization, $P(x)$, calculated for a fixed bilayer hydration potential, $\psi_{hyd} = 0.6$ V, orientational susceptibility, $\chi = 8.8 \cdot 10^{-12}$ A · s · (V · m)$^{-1}$, and water-order correlation length, $\xi = 0.25$ nm, and for various values of the water-layer thickness, $d_w = 0.22, 0.44, 0.66, 0.88$, and 1.1 nm.

ations that can, however, give an estimate of the size of various molecular parameters associated with F_P.

The most obvious electrostatic contribution to F_P is that of surface dipoles. We, therefore, model each isolated head-group layer as a sandwich of two oppositely charged planes (carrying net surface charge densities $+\sigma$ and $-\sigma$, respectively) and then identify F_P with the corresponding electric field. If we now let both charged planes coalesce, yielding a flat surface of uniform dipolar density with normal component τ_P, it follows that $P(\pm d_w/2 \rightarrow \infty) = (\epsilon - 1)\tau_P/\epsilon\xi$ (Cevc, G., B. Žekš, and R. Podgornik, manuscript in preparation). If we neglect electronic and intermolecular polarization $\chi = \epsilon_o(\epsilon - 1)/\epsilon$, then we get $\psi_{hyd} = \tau_P/\epsilon_o$. Similar arguments could also be used to estimate the contributions of higher multipoles to ψ_{hyd} and thus to F_P.

However, apart from the interactions between the surface multipoles and water dipoles, other possible origins of water polarization must not be forgotten. Probably, the most important is the existence of very short-range mutual electrostatic interactions between the local excess charges on the water and lipid molecules, such as are those involved in hydrogen-bond formation and its associated charge transfer process.

To simply model this interaction we use the fact that in electrostatic language the polarization can also be expressed in terms of the excess charge density. In the absence of interbilayer coupling the polarization, $P(d_w \rightarrow \infty)$, becomes directly proportional to the interfacial hydration capability so that we may by inverting Eq. 5 define the hydration potential as $\psi_{hyd} = (\xi\sigma_P/\epsilon_o)$, where $\sigma_P = -P(\pm d_w/2 \rightarrow \infty)\epsilon/(\epsilon - 1)$. In fact, this surface excess charge σ_P needs to be only locally different from zero because it only acts directly across very short distance, e.g., between the atoms on lipid and/or water molecules. Nevertheless, once σ_P has perturbed the solvent dipoles, its effect extends over a distance of the order of the water-polarization correlation length, ξ, due to the interwater coupling.

For phosphatidylethanolamine (and most other glycerophospholipids) the surface multipoles as well as the local excess surface charge can contribute to F_P and we therefore write ψ_{hyd} in a general form

$$\psi_{hyd} = (\xi/\epsilon_o)\,(\sigma_P + \tau_P/\xi + \nu_P/\xi^2 + \ldots),$$

where ν_P is the surface density of the quadrupole moment and the series extends over all nonzero multipole densities.

The relation between σ_P (or τ_P/ξ) and ψ_{hyd} resembles the solution of the linearized Poisson-Boltzmann equation for the electrostatic potential of a surface in contact with a nonpolarizable electrolyte solution, where ξ replaces the Debye screening length (28, 31) and σ_P appears instead of the net surface charge density. This correspondence offers an interpretation of Eq. 5: As two polar surfaces approach, the local excess surface charges or normal dipolar components at both interfaces become subject to mutual, polarization- (i.e., water-) mediated screening. The effective surface density of local excess charge then becomes dependent on the interlamellar spacing: $\sigma_P(d_w) = \sigma_P(d_w \rightarrow \infty)\tanh(d_w/2\xi)$, and a similar expression also holds for the normal dipolar component (Cevc, G., B. Žekš, and R. Podgornik, manuscript in preparation). Our boundary condition then means that the bilayer surface hydration potential is considered constant, whereas the results of Marčelja and co-workers (15, 16, 20, 28) would be valid if σ_P = constant.

Free Energy, Enthalpy, and Entropy of Hydration

Because of the simple form of $F_P(x)$, Eq. 1 reduces (by integration by parts of the $[dP/dx]^2$ term) to an expression that contains solely one surface integral

$$G^{hyd}(d_w) = -\psi_{hyd}\oint P(x) \cdot dS. \qquad (6)$$

The use of Eq. 5 for $P(x)$, then leads to the expression for the total free energy of hydration of the two similar, mutually interacting bilayer surfaces

$$G^{hyd}(d_w) = -(\chi S\psi_{hyd}^2/\xi)\tanh(d_w/2\xi), \qquad (7)$$

where S is the surface area per mole of the mutually interacting surfaces. This total free energy of hydration is the sum of the self-free energy of hydration, $G^{hyd}(d_w \rightarrow \infty) = G_\infty^{hyd}$, of the isolated surfaces

$$G_\infty^{hyd} = -(\chi S\psi_{hyd}^2/\xi) \qquad (8)$$

and the hydrational interaction free energy of the two surfaces

$$G_{int}^{hyd}(d_w) = -(\chi S\psi_{hyd}^2/\xi)\,[\tanh(d_w/2\xi) - 1] = G_\infty^{hyd}\,[\tanh(d_w/2\xi) - 1]. \qquad (9)$$

Thus, the energy of interaction, $G_{int}^{hyd}(d_w)$, gradually approaches the negative value of the self-energy terms, as the interbilayer separation tends to zero. Finally, for $d_w = 0$, $G_{int}^{hyd}(0) = -G_\infty^{hyd}$ and the interactions of the two opposing lamellae exactly cancel, i.e., for a single water molecule embedded between the two lamellae the opposing forces from the two surfaces counterbalance and the molecule remains unbound.

The entropy of hydration can be calculated from the free energy using the standard expression $S = -(\partial G/\partial T)$. Thus, from Eq. 7

$$S^{hyd}(d_w) = \{(\partial \ln G_\infty^{hyd}/\partial T) + [d_w/\xi \sinh(d_w/\xi)]\,\partial \ln(d_w/\xi)/\partial T\}G^{hyd}(d_w), \qquad (10)$$

which simplifies for $d_w >> \xi$ to

$$S^{hyd}(d_w) \simeq (\partial G_\infty^{hyd}/\partial T)\tanh(d_w/2\xi) \simeq S_\infty^{hyd}\tanh(d_w/2\xi). \qquad (11)$$

Similarly, the enthalpy of hydration of the bilayer, $H^{hyd}(d_w) = G^{hyd}(d_w) + TS^{hyd}(d_w)$, is given by

$$H^{hyd}(d_w) \simeq H_\infty^{hyd}\tanh(d_w/2\xi), \qquad (12)$$

where the enthalpy corresponding to infinite separation is: $H_\infty^{hyd} = G_\infty^{hyd} + T \cdot S_\infty^{hyd}$.

Interbilayer Hydration Force

The interbilayer repulsive pressure arising from the surface polarization of the water molecules is by the definition $p_{rep}^{hyd}(d_w) = (1/S)\,(\partial G_{int}^{hyd}[d_w]/\partial d_w)$. Hence from Eq. 9

$$p_{rep}^{hyd}(d_w) = -(\chi\psi_{hyd}^2/2\xi^2)\,\mathrm{sech}^2(d_w/2\xi), \qquad (13)$$

which indicates that the repulsive pressure is proportional to the square of the average water interfacial hydration potential. For relatively large separation $d_w >> \xi$, Eq. 13 may be approximated to

$$p_{rep}^{hyd} \simeq -(2\chi\psi_{hyd}^2/\xi^2)\exp(-d_w/\xi) \qquad (14)$$

implying an exponential dependence of the hydration repulsive force on bilayer separation. Eq. 14 agrees with the corresponding limiting expression derived by Marčelja and Radić (15) if we equate $(2\chi\psi_{hyd}^2/\xi^2) = 4\epsilon_o$. For small separations, $d_w \to 0$, then $\mathrm{sech}^2(d_w/2\xi) \to 1$ and the interbilayer repulsion approaches a constant value: $p_{rep}^{hyd} \simeq -\chi\psi_{hyd}^2/2\xi^2$. It should be remarked here that experiments (5) have already shown an approximately exponential dependence of $p_{rep}^{hyd}(d_w)$ with a tendency to level off as $d_w \to 0$.

Bilayer Phase Transition Energetics and Hydration-induced Transition Temperature Shifts

It is assumed that the water polarization decay length and the orientational susceptibility of the interlamellar water are both properties solely of the water subphase. Thus, the free energy of hydration changes at the phase transition only as a consequence of the change in the bilayer hydration potential $\Delta\psi_{hyd,t}$, and the change in lipid molecular area, ΔS_{Lt}, at T_t. Expanding up to second order in $\Delta\psi_{hyd,t}$ and ΔS_{Lt}, the change in hydration free energy at T_t is

$$\begin{aligned}\Delta G_t^{hyd}(n_w) = {} & (\partial G^{hyd}/\partial\psi_{hyd})\Delta\psi_{hyd,t} \\ & + (1/2)\,(\partial^2 G^{hyd}/\partial\psi_{hyd}^2)\Delta\psi_{hyd,t}^2 \\ & + (\partial G^{hyd}/\partial S_L)\Delta S_{Lt} \\ & + (1/2\,(\partial^2 G^{hyd}/\partial S_L^2)\Delta S_{Lt}^2 \\ & + (\partial^2 G^{hyd}/\partial\psi_{hyd}\partial S_L)\Delta\psi_{hyd,t}\Delta S_{Lt}. \qquad (15)\end{aligned}$$

Substituting from Eq. 7 and using the expression $d_w = 2n_wV_w/S_L$ (where $V_w \simeq 3.10^{-29}$ m^3 is the volume of one water molecule), the change in free energy of hydration at the phase transition becomes

$$\begin{aligned}\Delta G_t^{hyd}(n_w) = {} & G^{hyd}(n_w)\,\{[(2\Delta\psi_{hyd,t}/\psi_{hyd})\,(1 + \Delta S_{Lt}/S_L) \\ & + \Delta S_{Lt}/S_L + (\Delta\psi_{hyd,t}/\psi_{hyd})^2] \\ & - (2n_wV_w/\xi S_L)\,\mathrm{csch}\,(2n_wV_w/\xi S_L) \\ & \cdot [1 + 2\Delta\psi_{hyd,t}/\psi_{hyd} + (n_wV_w/\xi S_L)\tanh \\ & (n_wV_w/\xi S_L)\cdot(\Delta S_{Lt}/S_L)]\,(\Delta S_{Lt}/S_L)\}. \qquad (16)\end{aligned}$$

Equivalent expressions hold for the hydration contributions to the transition enthalpy and transition entropy, $\Delta H_t^{hyd}(n_w)$ and $\Delta S_t^{hyd}(n_w)$, respectively. The dependence of ΔG_t^{hyd} on $\Delta\psi_{hyd,t}/\psi_{hyd}$ and on ξ is illustrated in Fig. 2 for $n_w = 12$ and $\chi\psi_{hyd}^2 = 3.1 \cdot 10^{-12}$ N (see later on). The solid line indicates the most probable dependence in the range of likely values of $\Delta\psi_{hyd,t}/\psi_{hyd}$ and ξ suggested by experiment (shaded region). The insert shows the values of the curly bracket in Eq. 16 as a function of $\Delta\psi_{hyd,t}/\psi_{hyd}$.

If the total free energy of the hydrated bilayer is written as $G \equiv G^{anhyd} + G^{hyd}$ and similarly for the enthalpy and the entropy, then the

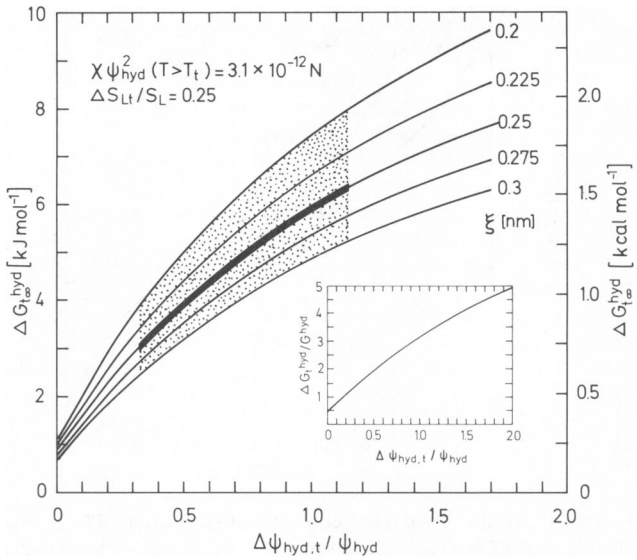

FIGURE 2 Change in bilayer hydration free energy, ΔG_t^{hyd}, at the chain-melting transition as a function of fractional change in the bilayer hydration potential $\Delta\psi_{hyd,t}/\psi_{hyd}$, at the transition, and for various values of the water polarization correlation length, ξ ($n_w = 12$, corresponding to complete hydration). Values of $\chi\psi_{hyd}^2(T > T_t) = 3.1 \cdot 10^{-12}$ N, $\Delta S_{Lt}/S_L = 0.25$ and $S_L \sim 0.55$ nm^2 were taken, based on the experiments. The shaded area represents the likely range of values of $\Delta\psi_{hyd,t}/\psi_{hyd}$, and ξ suggested by x-ray measurements and the solid line represents the most probable values. Insert shows $\Delta G_t^{hyd}/\Delta G^{hyd}$ for $\xi = 0.25$ nm.

change at T_t is given by

$$\begin{aligned}\Delta H(T_t) &\equiv \Delta H^{anhyd}(T_t) + \Delta H^{hyd}(T_t) \\ &= T_t[\Delta S^{anhyd}(T_t) + \Delta S^{hyd}(T_t)], \qquad (17)\end{aligned}$$

which uses the condition that the total free-energy change at a first-order transition is zero: $\Delta G(T_t) = 0$. Using Eq. 17, the hydration contribution to the free-energy change at the phase transition is then given by

$$\begin{aligned}\Delta G^{hyd}(T_t) &\equiv \Delta H^{hyd}(T_t) - T_t\Delta S^{hyd}(T_t) \\ &= T_t\Delta S^{anhyd}(T_t) - \Delta H^{anhyd}(T_t). \qquad (18)\end{aligned}$$

At the transition temperature of the anhydrous lipid, T_t^{anhyd}, the condition that the free-energy change is zero gives

$$\Delta H^{anhyd}(T_t^{anhyd}) = T_t^{anhyd}\Delta S^{anhyd}(T_t^{anhyd}), \qquad (19)$$

and then combining Eqs. 18 and 19

$$\Delta G^{hyd}(T_t) = T_t\Delta S^{anhyd}(T_t) - T_t^{anhyd}\Delta S^{anhyd}(T_t^{anhyd}). \qquad (20)$$

Experimentally, it is observed that the lipid-specific heats are approximately equal immediately above and below the transition temperature, and further that the specific heats and their temperature dependence are similar for different lipids on a reduced temperature scale (29, 30). Under these circumstances, the temperature dependence of ΔH and ΔS may be neglected, i.e., $\Delta H^{anhyd}(T_t^{anhyd}) = \Delta H^{anhyd}(T_t)$ and $\Delta S^{anhyd}(T_t^{anhyd}) = \Delta S^{anhyd}(T_t)$, (a similar result is also obtained if it is assumed that the specific heat is not temperature dependent). Hence, from Eq. 20 the hydration-induced shift in transition temperature is given by

$$\Delta T_t^{hyd}(n_w) \equiv (T_t - T_t^{anhyd}) = \Delta G_t^{hyd}(n_w)/\Delta S_t^{anhyd}, \qquad (21)$$

where ΔS_t^{anhyd} is the transition entropy of the anhydrous bilayer. Hence, the transition temperature shifts are calculated from Eqs. 16, 21. Because

ΔS_t^{anhyd} increases with increasing chainlength, the shifts will be less for the lipids with longer chains.

At the chain-melting transition, the area/lipid molecule increases: $\Delta S_{Lt} > 0$, since the fluid chains are more expanded. The affinity of the head groups for water should also increase at the transition, $\Delta\psi_{hyd,t} > 0$, because the polar residues then become more exposed. Because $G^{hyd}(n_w) < 0$ (cf. Eq. 7) and the second term in Eq. 16 is always smaller than the first, the transition temperature of the hydrated bilayers is always lower than that of the anhydrous lipid, i.e., $\Delta T_t^{hyd} < 0$.

The size of the second term in the bracket in Eq. 16 depends on the values of $\Delta\psi_{hyd,t}/\psi_{hyd}$ and $\Delta S_{Lt}/S_L$. Even in the worst case $\Delta\psi_{hyd,t}/\psi_{hyd} \sim 0.33$) it contributes <30% of the total at low water, $n_w \to 0$, and decreases to ~2% at limiting hydration. For $\Delta\psi_{hyd,t}/\psi_{hyd} = 1.16$, its contribution has decreased to ~12% and <1% at zero and limiting hydration, respectively. An approximate value for the transition temperature shift is thus given by

$$\Delta T_t^{hyd} \simeq -(\chi N_A S_L \psi_{hyd}^2/\xi \Delta S_t^{anhyd})\,[(2\Delta\psi_{hyd,t}/\psi_{hyd}) \cdot (1 + \Delta S_{Lt}/S_L) + \Delta S_{Lt}/S_L + (\Delta\psi_{hyd,t}/\psi_{hyd})^2] \cdot \tanh(n_w V_w/\xi S_L) \quad (22)$$

or

$$\Delta T_t^{hyd} \simeq \Delta T_{t\infty}^{hyd} \tanh(n_w V_w/\xi S_L), \quad (23)$$

where $\Delta T_{t\infty}^{hyd}$ is the transition temperature shift at limiting hydration. At low water contents, $(n_w V_w/\xi S_L) << 1$, and the following approximation holds

$$\Delta T_t^{hyd} \simeq \Delta T_{t\infty}^{hyd} (n_w V_w/\xi S_L). \quad (24)$$

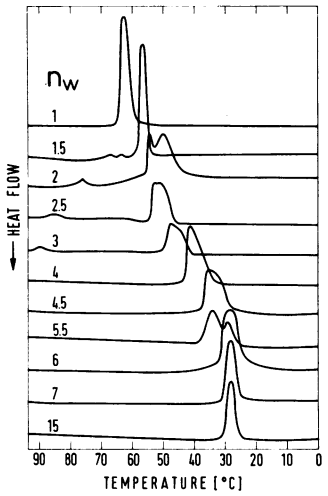

FIGURE 3 Differential calorimetric scans of 1,2-dilauroyl-*sn*-glycero-3-phosphoethanolamine (DLPE) at increasing water/lipid molar ratio, n_w. Cooling scans at 1.25 K · min^{-1}.

Thus, the transition temperature shift in the low hydration range is directly proportional to the number of water molecules per lipid. This is also true if the second term in Eq. 16 is retained. When the water content approaches limiting hydration, $(n_w V_w/\xi S_L) >> 1$, each subsequent water molecule that still binds to the phospholipid head group has a progressively diminishing effect on the transition. The transition temperature then asymptotically approaches the excess water value as $1-2\exp(-2n_w V_w/\xi S_L)$.

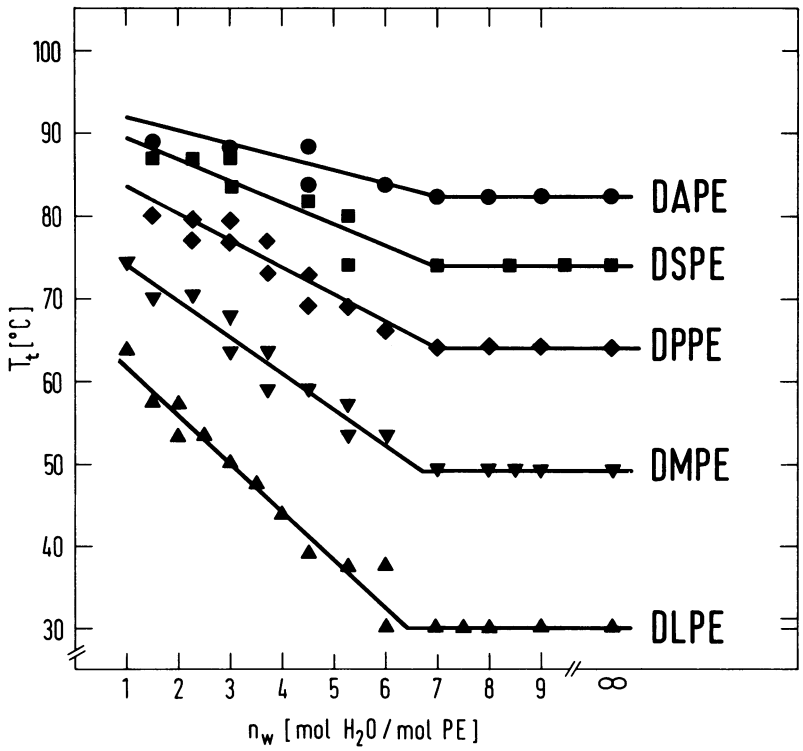

FIGURE 4 Calorimetrically determined phase transition temperatures of 1,2-diacyl-*sn*-glycero-3-phosphoethanolamines of increasing chainlength, as a function of water/lipid molar ratio, n_w. The transition temperature T_t corresponds to the major enthalpic peak in the cooling scan after temperature cycling to ensure reproducibility. The straight lines are drawn solely to guide the eye.

RESULTS

Differential Scanning Calorimetry

Cooling scans gave the simplest endotherms, presumably because of the known metastability and tendency to dehydrate of the phosphatidylethanolamine gel phase (21). If, however, the heating run was initiated close to the chain-melting transition, immediately after termination of the cooling run, reversibility was observed, indicating a conditional equilibrium, except at very low water contents. For longer chainlengths, any metastability is far less marked, but to minimize interference from these efffects, cooling data are presented throughout unless otherwise noted. Calorimetric curves for DLPE samples with water/lipid molar ratios ranging from 1 to 15 are shown in Fig. 3. Results from samples containing <1 water molecule/lipid were complex and are not included (cf. reference 19). It is possible that the first water of hydration may differ from the subsequent ones in its thermodynamic effects and binding.

Addition of water to the lipid, which was assumed to be originally the monohydrate, produces a gradual shift of the major calorimetric endotherm to lower temperatures. Besides this chain-melting transition, another transition or transitions of lesser enthalpy were regularly seen at higher temperature in the low hydration region (see Fig. 3). As discussed in detail elsewhere (14), these smaller endotherms, which — in contrast to the major endotherm — shift upwards in temperature with increasing hydration, correspond to transitions from the lamellar to the inverted hexagonal or other nonlamellar states. For the intermediate states of hydration, the major endotherm had a complex shape, revealing the presence of several unresolved transitions, presumably corresponding to states of differing hydration. In the low hydration region, these multiple peaks appeared to be roughly equidistant. This increased breadth and structure of the transition is generally expected since water is a true second component and thus the transition is not isothermal but occurs via a two-phase region in accordance with the phase rule.

The transition temperatures, T_t, of the major endothermic peaks are plotted as a function of water content in Fig. 4, for phosphatidylethanolamines with chainlengths ranging from C-12 (DLPE) to C-20 (DAPE). The stepwise nature of the transition shifts at low water is clear from Fig. 3 and also from Fig. 8, especially for the case of DLPE (see particularly the heating points of Fig. 8). As the phospholipid chainlength increases, the hydration-induced shifts become smaller, which is to be expected since the contribution of the chains becomes relatively more important. The transition temperature shifts reach a limiting value at a water content of ~7 waters/lipid, which is within experimental error independent of the phospholipid chainlength. This latter is also to be expected since the water molecules interact primarily with the phospholipid head groups and not with the chains. The total hydration-induced transition temperature shifts, ΔT_t^{exp}, for each chainlength are given in Table I, together with corresponding theoretical estimates calculated using Eqs. 16 and 17.

The total enthalpy, ΔH_t, of the chain-melting transition decreases with increasing hydration, as indicated in Fig. 5 *a* for phosphatidylethanolamines of three different chainlengths. The decrease is initially rapid at low water content and then asymptotically approaches a limiting value at ~7 waters/lipid molecule. Nearly the same form of the water dependence is observed for the different chainlengths, although the absolute values of ΔH_t are, of course, larger for the longer chainlengths. Very similar results are found for the water and chainlength dependence of the transition entropy, $\Delta S_t = \Delta H_t / T_t$, which is plotted in Fig. 5 *b*. The water dependence could be even somewhat larger than indicated in this figure, due to the possibility that some of the enthalpy may be hidden in the baseline of the broad transitions observed at low water contents.

The fact that very similar hydration profiles of the transition enthalpy are obtained for the different chainlengths indicates that the measurements are little affected by possible metastability of the low temperature phase, since this is known to be insignificant for the longer chainlength phosphatidylethanolamines (19). In addition, the absolute values of ΔH_t are considerably lower than observed for transition to a crystalline phase (19, 21). For the shorter chainlength PEs, the bilayer gel phase (L_β) is metastable, transforming on incubation to a crystalline phase (L_c) (see reference 21). However, the regularity of the data with increasing chainlength suggests that in all cases we are studying the equilibrium hydrational proper-

TABLE I
EXPERIMENTAL AND CALCULATED HYDRATION DEPENDENCE (n_w = 1 vs. n_w > 7) OF THE CHAIN-MELTING PHASE TRANSITION TEMPERATURE SHIFTS OF DIACYLPHOSPHATIDYLETHANOLAMINES

Chains	ΔT_t^{exp}	$\Delta S_t^{monohyd}$	ΔT_t^{calc}	
			ξ = 0.25 nm	ξ = 0.3 nm
	K	$J\,(mol \cdot K)^{-1}$	K	
C12	35	84.5	35 (48)	29 (40)
C14	26	111	26 (37)	22 (30)
C16	19.5	138	21 (29)	18 (25)
C18	13	170	17 (24)	14 (20)
C20	8.5	197	15 (21)	12 (17)

Experimental transition temperature shifts are obtained from cooling scans. Calculated transition temperature shifts are obtained from Eq. 17 with $\chi\psi_{hyd}^2 = 3.1 \cdot 10^{-12}$N at $T > T_t$, $\Delta S_{Lt}/\bar{S}_L = 0.25$, $S_L(T < T_t) = 0.42$ nm^2, $\Delta\psi_{hyd,t}/\bar{\Psi}_{hyd} = 0.5$, and using the full expression, Eq. 7, for $\Delta G_{t\infty}^{hyd} = G_\infty^{hyd}\,(T > T_t) - G_\infty^{hyd}\,(T < T_t)$. The values given in parentheses are calculated from the expansion for $\Delta G_{t\infty}^{hyd}$ of Eq. 16. Deviations between experimental and calculated shifts probably arise from neglecting the possible chainlength dependence of $\Delta\psi_{hyd,t}/\bar{\psi}_{hyd}$ and $\Delta S_{Lt}/\bar{S}_L$.

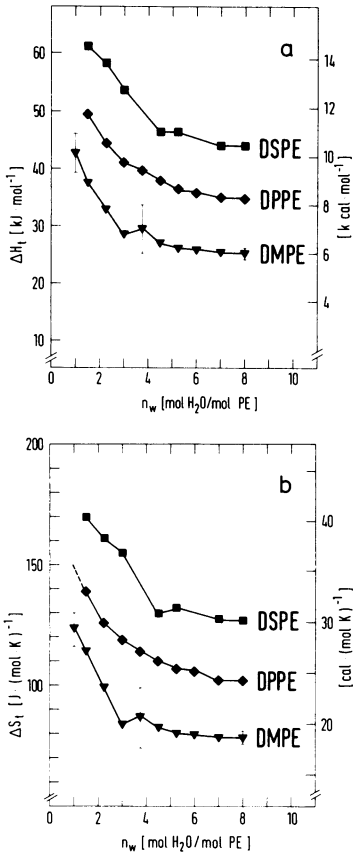

FIGURE 5 (*a*) Transition enthalpy and (*b*) transition entropy of 1,2-diacyl-*sn*-glycero-3-phosphoethanolamines of increasing chainlength as a function of water/lipid molar ratio, n_w. Determined from cooling scans at 1.25 K · min^{-1}.

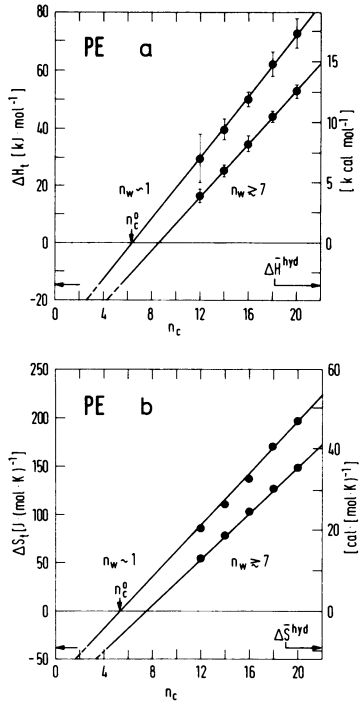

FIGURE 6 Chainlength dependence of (*a*) transition enthalpy ΔH_t and (*b*) transition entropy, ΔS_t, of almost anhydrous ($n_w \sim 1$) and fully hydrated ($n_w \gtrsim 7$) 1,2-diacyl-*sn*-glycero-3-phosphoethanolamines. $\Delta \bar{H}_t^{hyd}$ and $\Delta \bar{S}_t^{hyd}$ are the mean hydration contributions to ΔH_t and ΔS_t obtained from the difference of the two curves. The lines are linear least-squares fits.

ties of the gel-to-fluid bilayer phase transition, even though the former phase may be only conditionally stable for the shorter chainlengths.

The complete chainlength dependence of the transition enthalpy and the transition entropy for samples at greater than limiting hydration ($n_w \lesssim 7$), and for samples at low water content close to the monohydrate ($n_w \sim 1$), is given in Fig. 6. Both ΔH_t and ΔS_t increase approximately linearly with increasing chainlength, as discussed previously for the fully hydrated state (14). The chainlength dependences are almost parallel for the fully hydrated and low hydrated states, although a slight difference in slope cannot be excluded within the experimental error. The incremental transition enthalpy, $\partial \Delta H_t / \partial n_c$, is 4.66 ± 0.55 kJ/mol/$CH_2$ (1.1 ± 0.13 kcal/mol/CH_2) for $n_w \lesssim 7$, and 5.25 ± 2.1 kJ/mol/CH_2 (1.25 ± 0.5 kcal/mol/CH_2) for $n_w \sim 1$. The incremental transition entropy, $\partial \Delta S_t / \partial n_c$, is 11.8 ± 1.5 J/mol/K/$CH_2$ (2.8 ± 0.37 cal/mol/K/CH_2) and 13.5 ± 6 J/mol/K/CH_2 (3.2 ± 6 cal/mol/K/CH_2) for $n_w \lesssim 7$ and $n_w \sim 1$, respectively.

As a measure of the hydration contributions to the transition enthalpy and transition entropy, the values for the hydrated states are considered relatively to the values

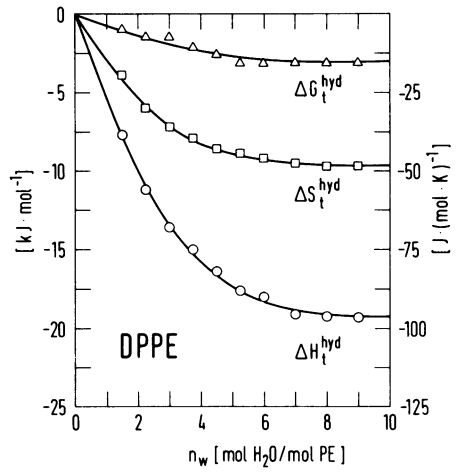

FIGURE 7 Hydration contribution to the transition free energy, ΔG_t^{hyd}, entropy, ΔS_t^{hyd}, and enthalpy, ΔH_t^{hyd}, as a function of water/lipid molar ratio, n_w, for DPPE. The values at zero hydration were estimated by extrapolation from the samples at low hydration, and were set equal to zero. The solid lines represent the theoretical calculations using water-order correlation lengths of ξ = 0.26, 0.24, and 0.26 nm for ΔG_t^{hyd}, ΔS_t^{hyd}, and ΔH_t^{hyd}, respectively.

for samples in the low hydration state with $n_w \sim 1$. In this way the possibly anomalous properties of the first water of hydration are avoided. The mean total hydration contributions to the transition enthalpy $\Delta\bar{H}_t^{hyd} = -16.1$ kJ/mol (3.85 kcal/mol), and to the transition entropy, $\Delta\bar{S}_t^{hyd}$ -38.3 J/mol/K (9.16 cal/mol/K), defined in this way are indicated in Fig. 6.

The dependence of the hydration contributions ΔH_t^{hyd} and ΔS_t^{hyd} as a function of water content for DPPE is given in Fig. 7, together also with the hydration free energy: $\Delta G_t^{hyd} = \Delta H_t^{hyd} - T_t \Delta S_t^{hyd}$. The form of the hydration dependence of ΔG_t^{hyd}, ΔH_t^{hyd}, and ΔS_t^{hyd}, in Fig. 7 is established with reference to the low hydration state, $n_w \sim 1$, and the zero values are obtained by fitting to Eq. 16 and corresponding expressions for ΔH_t^{hyd} and ΔS_t^{hyd}. The variation in all three thermodynamic quantities is again greatest at lower water contents and tends asymptotically to a limiting value at $\lesssim 7$ waters/lipid molecule. The total hydration contributions to the transition enthalpy and entropy are an appreciable fraction of the total values for the chain melting of the anhydrous lipid: $\Delta H_t^{hyd}/\Delta H_t^{anhyd} \sim \Delta S_t^{hyd}/\Delta S_t^{anhyd} \sim -1/3$, whereas the free-energy contribution and hence the transition temperature shift is relatively small, resulting from partial enthalpy-entropy compensation. It ranges between -3 and -1.7 kJ $\cdot$ mol^{-1} for DLPE and DAPE, respectively.

X-ray Diffraction

The calorimetrically determined phase transitions were, routinely in the case of DLPE and occasionally with the other PEs, confirmed by x-ray diffraction continuous temperature scans to correspond to the chain-melting phase transition.

The long spacings for DLPE above the phase transition were measured to be $d(n_w \gtrsim 7) \sim 4.6$ nm and $d(n_w \sim 2) \sim 3.55$ nm for the fully hydrated state and the state of low hydration, respectively. The corresponding values below the transition are: $d(n_w \gtrsim 7) \sim 5.0$ nm and $d(n_w \sim 1) \sim 4.5$ nm. The interlamellar water-layer thickness was calculated from these long spacings according to: $d_w = d(n_w \gtrsim 7) - d(n_w \sim 1, 2) + 0.1$ nm, where the additional 0.1 nm corresponds to the contribution of the residual water in the low hydration state at $T < T_t$. This water-layer thickness was thus found to be: $d_w(T < T_t) \sim 0.5 \pm 0.4$ nm below the chain-melting transition, and $d_w(T > T_t)$ 1.2 ± 0.08 nm above the transition. The short spacings measured below the chain-melting transition were ~ 0.42 nm, and the molecular area calculated from this chain-chain spacing was found to be $S_L(T < T_t) \sim 0.41$ nm^2 for all PEs studied. The area/molecule above the transition was taken from reference 19 to be $S_L(T > T_t) \sim 0.55$ nm^2. The limiting hydration numbers corresponding to these values for DLPE are $n_{wL}(T < T_t) \sim 3.5 \pm 3$ H_2O/PE below the transition, and $n_{wL}(T > T_t) \sim 11 \pm 1$ H_2O/PE above the transition, the former being biased towards lower limiting hydration due to the known metastability and tendency to dehydrate of the short chainlength PEs (see reference 19).

The dependence of the measured water-layer thickness on water content for DLPE in the fluid phase was used to determine the bilayer-bilayer interaction forces using the methods of references 5–7. The water activity corresponding to the various water contents, required for this calculation, was obtained from the adsorption isotherms of reference 22. The accuracy of the determinations is limited by the difficulty in correcting the adsorption isotherms to a reduced temperature scale. Furthermore, the presence of several x-ray reflections that did not correspond to lamellar phases, particularly at lower water contents, seriously hampered the interpretation of the results. Therefore, the results were analyzed only over the range of higher water contents: $n_w \sim 5$–9. The best fit through the data points for the fluid phase of DLPE yielded an approximately exponential decrease in the interbilayer repulsion, with a water-order correlation length: $\xi \sim 0.25 \pm 0.05$ nm, which had little temperature dependence to within our experimental accuracy. Assuming that the bilayer repulsion is written as: $p_{rep}^{hyd}(d_w) = p_o \cdot e^{-d_w}/\xi$, the extrapolated value at the surface was: $p_o = 10 \pm 1) \cdot 10^7$ N $\cdot$ m^{-2} for the fluid phase. A similar result was also obtained by assuming a fixed area/molecule: $S_L \sim 0.48$ nm^2, in order to use the water content, n_w, to calculate the water-layer thickness, d_w, and then combining this with the adsorption isotherm from reference 22.

Below the transition, the presence of additional x-ray reflections and a lack of the relevant adsorption isotherm data precluded a similar analysis of the bilayer-bilayer interaction forces. Instead the hydration contribution to the total force was calculated from the equilibrium water-layer thickness at full hydration. It was assumed that the Hamaker constant was the same as that determined from the DLPE fluid phase data: $H(T > T_t) \sim 24.10^{-21}$ J, in order to evaluate the contribution from the van der Waals interaction (see references 5–7). The effective value for the hydration repulsion at the bilayer surface was thus estimated to be $6.6 \cdot 10^6$ N $\cdot$ m$^{-2} \leq p_o < 5.2 \cdot 10^7$ N $\cdot$ m^{-2} for DLPE below the chain-melting transition. More details of the x-ray diffraction measurements on phosphatidylethanolamines have been published elsewhere (19).

DISCUSSION

The results of Figs. 3 and 4 and particularly the heating data in Fig. 8 suggest a stepwise hydration of the phosphatidylethanolamine molecules, whereby each of the various calorimetric peaks correspond to the chain melting of bilayer regions in which the degree of hydration differs by one water molecule per lipid. Similar results have recently been observed also for phosphatidylcholines (12). From the temperature increments and the measured transition entropies, it is possible to estimate the hydration contribution to the change in free energy at the phase transition

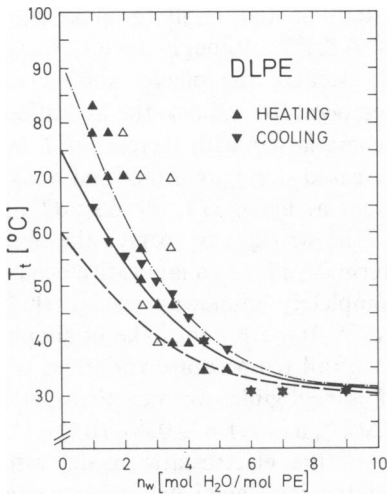

FIGURE 8 Experimental (Δ,∇) and calculated (lines) dependence of the chain-melting transition temperature, T_t, of DLPE on water/lipid molar ratio, n_w. Open symbols denote minor calorimetric peaks or peaks that disappear upon repeated temperature cycling. The solid line was calculated for $\Delta G_{t\infty}^{hyd} = -4.6$ kJ · mol^{-1}, and correlation length, $\xi = 0.25$ nm, suggested by the x-ray diffraction results, together with the extrapolated value $\Delta S_t^{anhyd} = 105$ J(mol · K)$^{-1}$. The dashed and dashed-and-dotted lines were obtained using the lower and upper limits for $\Delta G_{t\infty}^{hyd}$: −2.9 kJ · mol^{-1} and −6.3 kJ · mol^{-1}, respectively, implied by the x-ray diffraction results.

TABLE II
EXPERIMENTAL AND THEORETICAL ESTIMATES OF THE HYDRATION FREE ENERGY OF PHOSPHATIDYLETHANOLAMINE

n_w	ΔG_t^{exp}	ΔG_t^{exp}	G_{PCILO}	G_{SCF}	G_{MC}	$G_C(n_w, \xi)$
	kJ mol^{-1}			*percent*		
1	−1.5	21	19	19	31	37
2	−1.31	18	15	18	29	28
3	−1.31	18	14	16	10	15
4	−1.05	14.7	14	14	8	9
5	−0.79	11	12	13	5	6
6	−0.52	7.3	9	11	4	3
7	−0.4	5.5	7.5	(8)	3	1.5
8	−0.26	3.7	4	—	3	1
9	—	—	4	—	2	1
1	(*kJ · mol*$^{-1}$)	−1.5	−108.4	−119.5	−38.8	−2.04

Values give the contribution of the n_wth water molecule and are expressed as a percentage of the total, unless otherwise indicated. Bottom line gives absolute values for the 1st water molecule in kJ · mol^{-1}. $\Delta G_t^{exp} = \Delta T_t^{inc}$. ΔS_t^{anhyd} is the experimental change at T_t, measured from heating scans, for DLPE (see Fig. 8) and using the measured values for the increments ΔT_t^{inc} and the extrapolated value: $\Delta S_t^{anhyd} = 105$ J · (mol · K)$^{-1}$. All other values represent net free energies. G_{PCILO} and G_{SCF} are quantum mechanical calculations of the binding of single water molecules to dimethylphosphate, from references 26 and 27, respectively. G_{MC} is the result of a Monte Carlo calculation of the interaction of water molecules with a hexagonal lattice of phosphatidylethanolamine head groups from reference 23. These free energies are rearranged in descending order of their absolute values. $G_C(n_w, \xi)$ are calculations from the present continuum model (Eq. 7) with $\chi\psi_{hyd}^2 = 3.1 \cdot 10^{-12}$ N, $S_L = 0.55$ nm^2, and $\xi = 0.26$ nm.

from each successive water molecule. These results are given in Table II, which illustrates the progressively decreasing contributions of subsequent water molecules, as has been found in theoretical estimates of the binding energy of water molecules to phospholipid head groups (23). In principle, if the binding energies of the individual water molecules in both states are known, all the thermodynamic properties can be calculated using the methods of statistical mechanics. A first attempt at this approach has already been made (24) by using the water-binding isotherm to estimate the binding energies. However, the whole of the binding energy was assigned to the first layer of water molecules, and here we have instead used a continuum model to estimate the binding energies of the various water layers.

The approach to the lipid hydration given in the Theory section treats the water binding to the polar head groups as an end effect that modulates the chain fluidity in an essentially nonchainlength-dependent manner. Because the lipid chains and polar head groups are a coupled system, which involves also the water molecules, this is clearly only a first approximation and a fuller treatment would require minimizing the energy of the total system not just a single part. However, the approximate treatment as an end effect has experimental justification, since there is only a relatively small variation in ΔH_t^{hyd} and ΔS_t^{hyd} with chainlength as shown in Fig. 6. Furthermore, the slope of the water dependence of the transition temperatures in Fig. 4 decreases with increasing chainlength, approximately proportional to $1/\Delta S_t^{anhyd}$ as predicted by the perturbation treatment of Eq. 21. This can be seen also from the chainlength dependence of the calculated theoretical shifts in Table I.

The water dependence of the thermodynamic properties of the phosphatidylethanolamine chain-melting transition can be described very well by the model given above. The hydration dependence of ΔG_t^{hyd}, ΔH_t^{hyd}, and ΔS_t^{hyd} for DPPE (Fig. 7) can be fitted by expressions analogous to the approximate Eq. 23: $\Delta G_t^{hyd} = \Delta G_{t\infty}^{hyd} \tanh(n_w V_w/\xi S_L)$, etc., with $\Delta G_{t\infty}^{hyd} = -3.0$ kJ/mol and water-order correlation length $\xi = 0.30$ nm; $\Delta H_{t\infty}^{hyd} = -19.3$ kJ/mol and $\xi = 0.26$ nm; and $\Delta S_{t\infty}^{hyd} = -48.3$ J/mol/K and $\xi = 0.24$ nm. All these characteristic correlation lengths are of a similar order of magnitude and are close to that obtained from the bilayer-bilayer interaction forces by x-ray diffraction. Inclusion of the additional terms in Eq. 16 gives an equivalent fit (for $\Delta\psi_{hyd,t}/\psi_{hyd} = 0.66$ and $\Delta S_{Lt}/S_L = 0.25$, see below), but with slightly altered correlation lengths: $\xi = 0.25$ nm for ΔG_t^{hyd}, 0.22 nm for ΔH_t^{hyd} and 0.20 nm for ΔS_t^{hyd}.

The comparison of the theory with the water dependence of the experimental transition temperature shifts of DLPE is given in Fig. 8. Good fits can be obtained to the hyperbolic tangent dependence predicted by Eq. 23 with

the shift at limiting hydration $\Delta T_{t\infty}^{hyd} = -79°C$ and water polarization decay length $\xi = 0.3$ nm for the heating runs, and $\Delta T_{t\infty}^{hyd} = -43°C$ and $\xi = 0.22$ nm for the cooling runs (curves not shown). Alternatively, the full expression from Eq. 16 may be used with parameter values suggested by x-ray diffraction.

The water-ordering model presented in the Theory section is thus capable of describing the functional form of the water dependence of the chain-melting transition for phosphatidylethanolamines, even down to very low water contents. The characteristic correlation length for the water polarization is essentially the same as that estimated from our x-ray diffraction experiments and from those of others (6). Further comparison with the diffraction results also allows a check on whether the magnitudes of the thermodynamic shifts are consistent with the observed hydration forces. From the measured bilayer-bilayer repulsion together with the correlation length $\xi \sim 0.25$ nm, it can be estimated that $2.1 \cdot 10^{-13}\ N \leq \chi\psi_{hyd}^2(T < T_t) \leq 1.6 \cdot 10^{-12}\ N$ below the transition, and $\chi\psi_{hyd}^2(T > T_t) > 3.1 \cdot 10^{-12}\ N$ above the transition. Hence, assuming $\chi \sim 8.8\ 10^{-12}$ N, the change in the bilayer hydration potential at the phase transition is $0.33 \leq \Delta\psi_{hyd,t}/\psi_{hyd} \leq 1.16$, and the expansion in area/molecule is $\Delta S_{Lt}/S_L \sim 0.25$, as found from the x-ray measurements. From Eq. 16 these values give the following estimate for the total hydration contribution to the transition free energy: $-6.3\ kJ \cdot mol^{-1} \leq \Delta G_{t\infty}^{hyd} \leq -2.9\ kJ \cdot mol^{-1}$, which is in good agreement with the experimental value for DPPE deduced from Fig. 7. The total hydration-induced transition temperature shift can also be estimated from Eqs. 16 and 17. For DLPE $-62.5°C \leq \Delta T_{t\infty}^{hyd} \leq -30°C$, which is in reasonable agreement with the extrapolated experimental value for the cooling scans, $\Delta T_{t\infty}^{hyd} \sim -43°C$ from Fig. 8. Using the correlation length $\xi \sim 0.25$ nm, the water dependence of the transition temperatures obtained from the cooling runs are well fit with $\chi\psi_{hyd}^2 = 1.7 \cdot 10^{-12}$ N and $\Delta\psi_{hyd,t}/\psi_{hyd} = 0.66$ (full line in Fig. 8), which is also relatively close to the measured averages $\chi\psi_{hyd}^2 = 2.1 \cdot 10^{-12}$ N and $\Delta\psi_{hyd,t}/\psi_{hyd} = 0.82$. The heating data are reasonably well fit by the upper limit values (dashed-and-dotted line in Fig. 8), whereas the lower limit values predict shifts that are too small.

The changes at the chain-melting transition are therefore principally due to the increase in hydration potential, ψ_{hyd}, and in the molecular area, S_L, the former being considerably the greater. Thus, it becomes clear that the main origin of the hydration-induced phase transition shift is the increased ability of the phosphatidylethanolamine lipid to bind water at $T > T_t$.

To make estimates of the absolute values of ΔH_t^{hyd} and ΔS_t^{hyd}, information is required as to the temperature dependence of the terms $\chi S\psi_{hyd}^2/\xi$ in Eq. 12. We have seen that if one assumes a purely electrostatic model that involves solely orientational water polarization, then $\chi = \epsilon_o(\epsilon - 1)/\epsilon$, where ϵ is the dielectric constant of interlamellar water. With the experimental values of $\partial\epsilon/\partial T$ for bulk water, this term is too small to make an appreciable contribution to ΔS_t^{hyd}, although the interfacial value may be different. Because the bilayer surface expands with increasing temperature and also the hydration potential is likely to become larger with increasing T (as concluded from the decreased steric hindrance and weakened interlipid interactions at higher T), the $\partial S_L/\partial T$ and $\partial\psi_{hyd}/\partial T$ terms are of the wrong sign to give the observed ΔS_t^{hyd}. Hence, the term $\partial\xi/\partial T$, the quantitative behavior of which is to date completely unknown, must be the main determinant of ΔS_t^{hyd}. If we for the sake of simplicity assume that the sum of all temperature variations of parameters other than ξ is negligible, we may then get $\xi^{-1}\ (\partial\xi/\partial T)$ from $\Delta S_t^{hyd}/\Delta G_t^{hyd}$; it is $-1.6 \pm 0.8 \cdot 10^{-2}\ K^{-1}$.

The use of the electrostatic model also allows an estimation of the interfacial hydration potential and its associated molecular electrostatic parameters, such as σ_P and τ_P. Taking $\epsilon = 80$ for the water dielectric constant gives a value $\chi \simeq 8.8 \cdot 10^{-12}\ A \cdot s(V \cdot m)^{-1}$ for the orientational susceptibility. Using the value from the measured repulsive pressure at $T > T_t$ of $\chi\psi_{hyd}^2 = 3.1 \cdot 10^{-12}$ N then yields $\chi_{hyd}(T > T_t) = 0.6$ V. It is these values of χ and ψ_{hyd} that were used in the calculation of the polarization profile in Fig. 1. Using the measured x-ray repeat distances at $T < T_t$ yields correspondingly $0.15\ V \leq \psi_{hyd}(T < T_t) \leq 0.42$ V.

For $\tau_P = 0$ this gives $\sigma_P(T > T_t) = 2.1 \cdot 10^{-2}\ A \cdot s \cdot m^{-2}$ ($0.13\ e/nm^2$) and $5.3 \cdot 10^{-3}\ A \cdot s \cdot m^{-2} \leq \sigma_P(T < T_t) \leq 1.5 \cdot 10^{-2}\ A \cdot s \cdot m^{-2}$. Taking, on the other hand, $\sigma_P = 0$ leads to $\tau_P(T > T_t) = 5.2 \cdot 10^{-12}\ A \cdot s \cdot m^{-1}$ and $1.3 \cdot 10^{-12}\ A \cdot s \cdot m^{-1} \leq \tau_P(T < T_t) \leq 3.7 \cdot 10^{-12}\ A \cdot s \cdot m^{-1}$. The corresponding values obtained from quantum-mechanical simulations of phosphatidylethanolamine lattices are $0 < \tau_P < 4.1 \cdot 10^{-11}\ A \cdot s \cdot m^{-1}$ for the normal component of the dipolar moment and $0.35\ A \cdot s \cdot m^{-2}$ for the excess surface charge density on the phosphate group as the primary lipid hydration site (23). Our values must be considered as rough upper limits; they differ from the simulated values in the case of σ_P by roughly one order of magnitude, a fact that is also apparent in the total values of G^{hyd} quoted in Table II, and possibly reflects the limited quantitative predictive power of quantum-chemical models for bilayers and/or the effect of the use of the linearized theory (31).

Although we have ignored the possible chainlength dependence of the hydration effects (since it is within our experimental error), it can be introduced by allowing the hydration potential to be chainlength dependent. This essentially would be the effect of minimizing the total bilayer energy, including both water and lipid chains. Empirically, the chainlength dependence can be allowed for by extrapolating the chainlength dependence to the chainlength, n_c^o, at which the ΔH_t or ΔS_t of the anhydrous lipid become zero (cf. Fig. 6). The extrapolation assumes that the nonhydrated head groups contribute relatively little to the thermodynamics of the transition, as evidenced by the fact that the differences in ΔH_t and ΔS_t between the

different phospholipid classes are very small compared with the effects of differing chainlength and/or hydration (cf. Fig. 5 and reference 25). The contribution of the chains alone thus becomes zero at n_c^o, i.e., this is the true chain end effect. From Fig. 6 $n_c^o \sim 5$–6, and at this chainlength the values of ΔH_t and ΔS_t at excess water are solely those due to hydration, and are close to those previously estimated.

In conclusion, the theory presented not only describes the water dependence of the calorimetric properties of the phosphatidylethanolamine chain melting, but also accurately predicts the order of magnitude of the hydration-induced effects. A consistent interpretation of the macroscopic calorimetric results with the x-ray data, which are obtained at the molecular level, is provided by the theory.

G. Cevc would like to thank B. Žekš and R. Podgornik for discussing some of the aspects of this work.

Received for publication 8 September 1983 and in final form 23 March 1984.

REFERENCES

1. Israelachvili, J. N., S. Marčelja, and R. G. Horn. 1980. Physical principles of membrane organization. *Q. Rev. Biophys.* 13:121–200.
2. Cevc, G. 1982. Water and membranes: the interdependence of their physico-chemical properties in the case of phospholipid bilayers. *Studia Biophysica.* 91:45–52.
3. Inoko, Y., and T. Mitsui. 1978. Structural parameters of dipalmitoylphosphatidylcholine lamellar phases and bilayer phase transitions. *J. Phys. Soc. Japan.* 44:1918–1924.
4. Janiak, M. J., D. M. Small, and G. G. Shipley. 1979. Temperature and compositional dependence of the structure of hydrated dimyristoyl lecithin. *J. Biol. Chem.* 254:6068–6078.
5. Parsegian, V. A., N. Fuller, and R. P. Rand. 1979. Measured work of deformation and repulsion of lecithin bilayers. *Proc. Natl. Acad. Sci. USA.* 76:2750–2754.
6. Lis, L. J., M. McAlister, N. Fuller, R. P. Rand, and V. A. Parsegian. 1982. Interactions between neutral phospholipid bilayer membranes. *Biophys. J.* 37:657–666.
7. Rand, R. P. 1981. Interacting phospholipid bilayers: measured forces and induced structural changes. *Annu. Rev. Biophys. Bioeng.* 10:237–314.
8. Chapman, D., R. M. Williams, and B. D. Ladbrooke. 1967. Physical studies of phospholipids. VI. Thermotropic and lyotropic mesomorphism of some 1,2-diacyl-phosphatidylcholines (lecithins). *Chem. Phys. Lipids.* 1:445–475.
9. Gottlieb, M. H., and E. D. Eanes. 1974. Coexistence of rigid crystalline and liquid crystalline phases in lecithin-water mesophases. *Biophys. J.* 14:335–342.
10. Ulmius, J., H. Wennerström, G. Lindblöm, and G. Arvidson. 1977. Deuterium nuclear magnetic resonance studies of phase equilibria in a lecithin-water system. *Biochemistry.* 16:5742–5745.
11. Luzzati, V., and F. Husson. 1962. The structure of the liquid-crystalline phases of lipid-water systems. *J. Cell Biol.* 12:207–219.
12. Kodama, M., M. Kuwabara, and S. Seki. 1982. Successive phase-transition phenomena and phase diagram of the phosphatidylcholine-water system as revealed by differential scanning calorimetry. *Biochim. Biophys. Acta.* 689:567–570.
13. Fisher, R. W., and T. L. James. 1978. Lateral diffusion of the phospholipid molecule in dipalmitoylphosphatidylcholine bilayers. An investigation using nuclear spin-lattice relaxation in the rotating frame. *Biochemistry.* 17:1177–1183.
14. Seddon, J. M., G. Cevc, and D. Marsh. 1983. Calorimetric studies of the gel-fluid (L_β-L_α) and lamellar-inverted hexagonal (L_α-H_{II}) phase transitions in dialkyl and diacyl phosphatidylethanolamines. *Biochemistry.* 22:1280–1289.
15. Marčelja, S., and N. Radić. 1976. Repulsion of interfaces due to boundary water. *Chem. Phys. Lett.* 42:129–130.
16. Marčelja, S. 1977. Structural contribution to solute-solute interaction. *Croat. Chem. Acta.* 49:347–358.
17. Cevc, G., B. Žekš, and R. Podgornik. 1981. The undulation of hydrated phospholipid multilayers may be due to water-mediated bilayer-bilayer interaction. *Chem. Phys. Lett.* 84:209–212.
18. Cevc, G., R. Podgornik, and B. Žekš. 1982. The free energy, enthalpy, and entropy of hydration of phospholipid bilayer membranes and their dependence on interfacial separation. *Chem. Phys. Lett.* 91:193–196.
19. Seddon, J. M., G. Cevc, R. D. Kaye, and D. Marsh. 1984. X-ray diffraction study of the polymorphism of hydrated diacyl- and dialkylphosphatidyl-ethanolamines. *Biochemistry.* 23:2634–2644.
20. Marčelja, S., D. J. Mitchell, B. W. Ninham, and M. C. Sculley. 1977. Role of solvent structure on solution theory. *J. Chem. Soc. Faraday Trans. II.* 13:630–648.
21. Seddon, J. M., K. Harlos, and D. Marsh. 1983. Metastability and polymorphism in the gel and fluid bilayer phases of dilauroyl phosphatidylethanolamine. Two crystalline forms in excess water. *J. Biol. Chem.* 258:3850–3854.
22. Jendrasiak, G. L., and J. C. Mendible. 1976. The effect of the phase transition on the hydration and electrical conductivity of phospholipids. *Biochim. Biophys. Acta.* 424:133–148.
23. Frischleder, H., and G. Peinel. 1982. Quantum-mechanical and statistical calculations on phospholipids. *Chem. Phys. Lipids.* 30:121–158.
24. Cevc, G., and D. Marsh. 1981. The contribution of the polar head group hydration to the phase transition of phospholipid bilayer membranes. *Period Biol.* 83:118–120.
25. Seelig, J. 1981. Thermodynamics of phospholipid bilayers. *In* Membranes and Intercellular Communication. Les Houches, 1979. R. Balian, M. Charbre, and P. F. Devaux, editors. North-Holland, Amsterdam. 36–54.
26. Frischleder, H., S. Gleichmann, and R. Krahl. 1977. Quantum-mechanical and empirical calculations on phospholipids. III. Hydration of the dimethyl-phosphate anion. *Chem. Phys. Lipids.* 19:144–149.
27. Pullman, B., A. Pullman, H. Berthod, and N. Gresh. 1975. Quantum-mechanical studies of environmental effects on biomolecules. VI. Ab initio studies on the hydration scheme of the phosphate group. *Theoret. Chim. Acta.* 40:93–111.
28. Gruen, D. W. R., and S. Marčelja. 1983. Spatially varying polarization in water. *J. Chem. Soc. Faraday Trans. II.* 79:225–242.
29. Wilkinson, D. A., and J. F. Nagle. 1982. Specific heats of lipid dispersions in single-phase regions. *Biochim. Biophys. Acta.* 688:107–115.
30. Blume, A. 1983. Apparent molar heat capacities of phospholipids in aqueous dispersion. Effects of chainlength and head group structure. *Biochemistry.* 22:5436–5442.
31. Cevc, G. 1985. Molecular force theory of solvation of the polar solutes. *In* Hydration Forces and Molecular Aspects on Solvation, Land 7089. B. Jönsson, H. Wennerström, and S. Forsen, editors. Cambridge University Press. In press.